Computational Analysis of Active Flow Control to Reduce Aerodynamics Drag on a Van Model

Harinaldi[a], Budiarso[b], Rustan Tarakka[c] and Sabar P. Simanungkalit[d]

Department of Mechanical Engineering Faculty of Engineering University of Indonesia, Kampus UI-Depok, , Jawa Barat, 16424, Indonesia

***Abstract*— Method of active flow control can be applied to reduce aerodynamic drag of the vehicle. It provides the possibility to modify locally the flow, to remove or delay the separation position or to reduce the development of the recirculation zone at the back as well as the separated swirling structures around the vehicle. In this study, a passenger van is modeled with a modified form of Ahmed's body by changing the orientation of the flow from its original form (modified/reversed Ahmed Body). This model is equipped with suction and blowing on the rear side to comprehensively examine the pressure field modifications that occur in order to modify the near wall flow toward reducing the aerodynamics drag. The computational simulation used is k-epsilon flow turbulence model. In this configuration, the front part of body was inclined at an angle of 35° with respect to the horizontal. The geometry is placed in a 3D-rectangular numerical domain with length, width and height equal to 8*l*, 2*l* and 2*l*, respectively. The suction and blowing velocities are set to 1 m/s, 5 m/s, 10 m/s and 15 m/s, respectively. The results show that aerodynamic drag reductions close to 15.83 % for suction and 14.38 % for blowing have been obtained.**

***Index Terms*— drag reduction, active flow control, suction, blowing, reversed Ahmed body.**

I. Introduction

According to the conclusions of International Energy Agency in World Energy Outlook 2007, the gas emissions with greenhouse effect will increase close to 57% in 2030 with strong effects on the environment and the climate [1]. The human activities became main cause of the increase of the greenhouse gases effect and average global temperature. The activities included the transportation sector where the growth number of automobile is rapidly increasing and make the fuel consumption increases as well. It tends to create harmful effects on the environment because it increases air pollution in the world. Based on these problems it has become a must for automobile industry in the world to immediately create an environmentally friendly automobiles and efficient in fuel consumption.

Fuel consumption of automobile is related to its aerodynamics drag, and the magnitude of aerodynamics drag is highly influenced by separation flows around its shape. Meanwhile, the flow around a traveling automobile is complex and presents nonlinear interactions between different parts of the automobile so that many research institutions and industrial laboratories have been focusing their investigations automotive aerodynamics with numerical studies [2]. It is necessary to modify locally the flow, to remove or delay the separation position or to reduce the development of the recirculation zone at the back and of the separated swirling structures. This can be mainly obtained by controlling the flow near the wall with or without additional energy using active or passive devices [3]. Significant results can be obtained using simple techniques [4,5].

Many active control techniques which have been developed by focusing on local intervention in wall turbulence deal with steady blowing or suction [6,7,8]. A blowing devices installed in an ONERA D profile can shift or even prevent the flow separation to occur [9]. A local suction system located on the upper part of the rear window is capable of eliminating the rear window separation on simplified fastback car geometry. Aerodynamic drag reductions close to 17% have been obtained [10]. Other numerical works [11] using Lattice Boltzmann method to an Ahmed body model indicated some important parameters of active control to improve the aerodynamics performance of a vehicle. Most of previous numerical study in flow around automobile's body used the geometry suggested by Ahmed [12] as shown in Fig. 1. Ahmed body allows reproducing flows phenomena around the vehicles and making a possibility to apply active control.

However, to be practically implemented in controlling the flow separation in the automotive application the active control methods still need further comprehensive investigations to obtain some fundamental insights of the governing mechanism of separation control. Hence, the current investigation was a part of a long-term fundamental

Manuscript received May 10, 2011. This work was supported by Incentive of Fundamental Research grant, The Ministry of Research and Technology Republic of Indonesia under contract no. RD-2011-0863

[a] Dr. Harinaldi is with the Department of Mechanical Engineering Faculty of Engineering University of Indonesia, Depok, Jawa Barat, 16424, Indonesia (Phone:+62-21-7270032;Fax:+62-21-7270033;e-mail:harinald@eng.ui.ac.id).

[b] Prof. Budiarso is with the Department of Mechanical Engineering Faculty of Engineering University of Indonesia, Depok, Jawa Barat, 16424, Indonesia (Phone:+62-21-7270032;Fax:+62-21-7270033;e-mail:mftbd@eng.ui.ac.id).

[c] Mr. Rustan Tarakka is a PhD student at the Department of Mechanical Engineering Faculty of Engineering University of Indonesia; e-mail: rustan_tarakka@yahoo.com

[d] Mr. Sabar P. Simanungkalit is a Master degree student at the Department of Mechanical Engineering Faculty of Engineering University of Indonesia; e-mail: sp.simanungkalit@gmail.com

investigation to develop an active control to the turbulent flow separation which is a fundamental phenomenon governing the aerodynamics performance of vehicle body. In this study, a passenger van is modeled with a modified form of Ahmed's body by changing the orientation of the flow from its original form (modified/reversed Ahmed Body). This model is equipped with suction and blowing on the rear side to comprehensively examine the pressure field modifications that occur in order to modify the near wall flow toward reducing of aerodynamics drag.

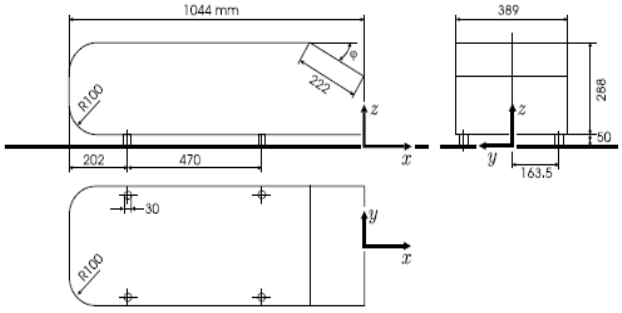

Fig 1. Original Ahmed model (dimensions in mm) [12]

II. MODELLING AND NUMERICAL SIMULATION

The numerical simulations presented in this paper were conducted on a modified/reversed Ahmed body which has geometrical ratio 0.25 to the original size. The model geometry was defined by its length (l = 0.261m), width (w = 0.09725 m) and its height (h = 0.072 m). In this configuration, the front part of body was inclined at an angle of 35^o with respect to the horizontal. The body is placed in a 3D rectangular numerical domain of length L = 8l, width W = 2l and height H = 2l as shown in Fig. 2.

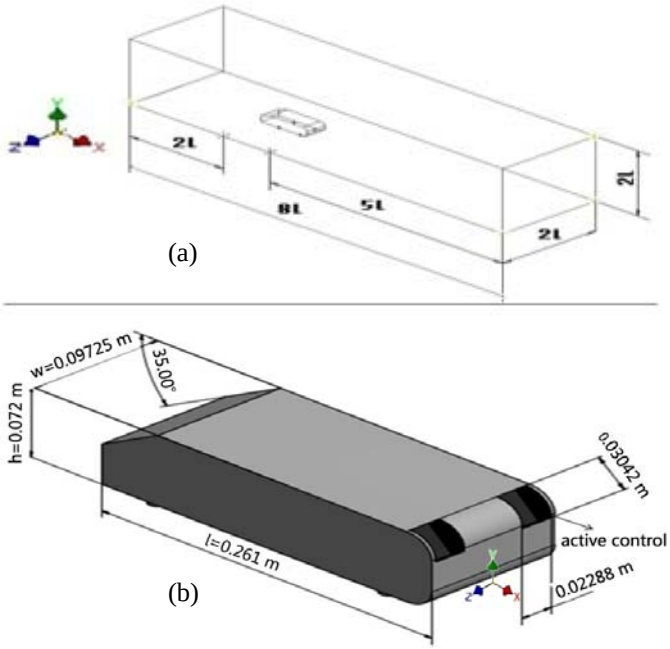

Fig 2. (a).Computational flow domain. (b).Geometrical dimensions of van model

The work was conduted by using a Gambit 2.4® software to generated the grid. Meshing type was tetra/hybrid element with hex core type and the grid number was more than 1.7 million in order to ensure detail discretization and more accurate calculation results. The boundary condition were inlet velocity of 16.7 m/s . Mean free stream at far upstream region was assumed in a steady state condition and uniform. The Reynolds number associated with length L of the geometry is Re = 2.98×10^5. The blowing and suction velocity are set 1 m/s, 5 m/s, 10 m/s and 15 m/s, respectively. Details of computation condition are given in Table 1.

Table 1. Computation condition

Computation Condition		
Model setting	3D, Steady state	
Fluid	Air	
Fluid properties	Density	1.225 kg/m^3
	Viscosity	0.000017894 kg/m-s
Boundary condition without flow control	Van model	Wall
	Pressure outlet	Pressure outlet
	Velocity inlet	Velocity inlet
	Wall	Wall
Boundary condition with suction/blowing	Van model	Wall
	Pressure outlet	Pressure outlet
	Velocity inlet	Velocity inlet
	Wall	Wall
	Suction1/blowing1	Velocity inlet
	Suction2/blowing2	Velocity inlet
Suction/blowing velocity	1 m/s , 5 m/s, 10 m/s and 15 m/s	

The governing equations were solved numerically by finite volume approach using a commercial solver Fluent 6.3® [13]. The turbulence model used in the computation was a standard k-epsilon model showed in Eq. (1) and (2)

$$\frac{\partial}{\partial t}(\rho k)+\frac{\partial}{\partial x_i}(\rho k u_i)=\frac{\partial}{\partial x_j}\left[\left(\mu+\frac{\mu_t}{\sigma_k}\right)\frac{\partial_k}{\partial x_j}\right]+G_k+G_b-\rho\varepsilon-Y_M+S_k \quad (1)$$

$$\frac{\partial}{\partial t}(\rho\varepsilon)+\frac{\partial}{\partial x_i}(\rho\varepsilon u_i)=\frac{\partial}{\partial x_j}\left[\left(\mu+\frac{\mu_t}{\sigma_\varepsilon}\right)\frac{\partial\varepsilon}{\partial x_j}\right]+C_{1\varepsilon}\frac{\varepsilon}{k}(G_k+C_{3\varepsilon}G_b)-C_{2\varepsilon}\rho\frac{\varepsilon^2}{k}+S_\varepsilon \quad (2)$$

where : $C_{1\varepsilon}$=1.44, $C_{2\varepsilon}$=1.92, C_μ=0.09, S_k =1.0, S_ε =1.3.

A dimensionless coefficient, called drag coefficient and related to the drag force acting on the bluff body, is defined as follows:

$$C_d=\frac{F_d}{\frac{1}{2}\rho V_\infty{}^2 S} \quad (3)$$

In this expression, ρ represents the air density, V_∞ is the free stream velocity, S is the cross section area and F_d is the total drag force acting on the car projected on the longitudinal direction. Note that the drag force F_d can be decomposed into a sum of a viscous drag force and a pressure drag force as:

$$F_d = \int \tau_w \sin\theta \, dS + \int p \cos\theta \, dS \quad (4)$$

Combining (3) and (4), the drag coefficient can be expressed as:

$$C_d = \int \frac{\tau_w}{\frac{1}{2}\rho V_\infty^{\,2} S} \sin\theta \, dS + \frac{\int C_p \cos\theta \, dS}{S} \quad (5)$$

Where $\tau_w = \mu(du/dy)_w$ is the wall shear stress evaluated from the wall velocity gradient and $C_p = (p-p_\infty)/(\rho V_\infty^{\,2}/2)$ is the pressure coefficient evaluated from the wall pressure distribution.

III. RESULTS AND DISCUSSION

A. Pressure Distribution

Some selected results from computational are described in the following figures. Fig. 3 shows computational result of the pressure coefficient distribution without flow control in the rear part of the reversed Ahmed body with the upstream velocity at 16.7 m/s evaluated at several span wise locations. From Fig. 3, it can be seen that the minimum value of pressure coefficient is -1.3819 at y/*h* = 1 and z/*w* = -1/12 in the rear side of the body.

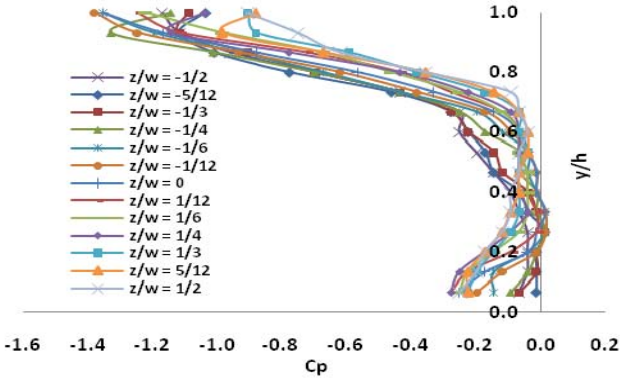

Fig 3. Pressure coefficient distribution without flow control in the rear part of the reversed Ahmed body

Meanwhile, Fig. 4 (a-d) describes the effect of various suction velocities in the rear part of the reversed Ahmed body to the pressure coefficient distribution with the upstream velocity at 16.7 m/s. The suction velocities are 1 m/s, 5 m/s, 10 m/s and 15 m/s. Closer insight to Fig. 4 (a-d) indicates that by introducing suction, the location of minimum value pressure coefficient shifted significantly to y/*h* = 1; z/*w* = -1/4 and y/*h* = 1; z/*w* = 1/4 in the rear side of the body. The minimum value of pressure coefficient is summarized in Table 2.

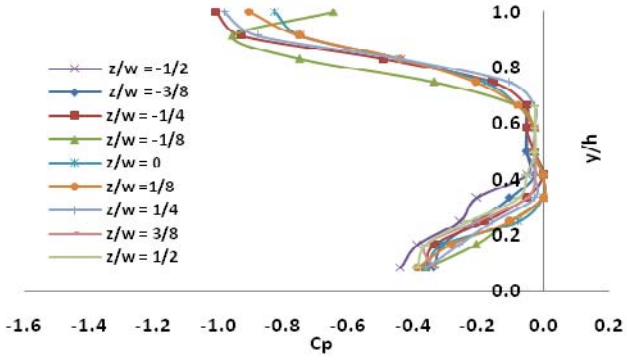

(a). Suction velocity, U_{sc} = 1 m/s

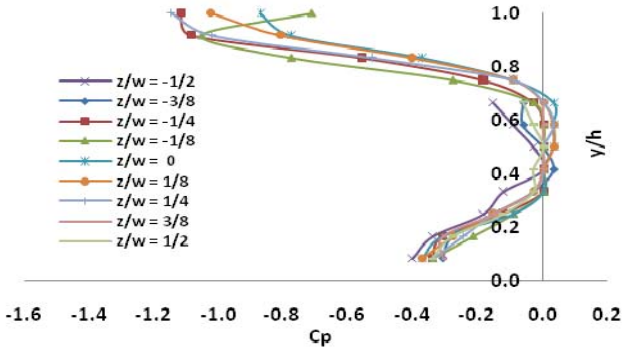

(b). Suction velocity, U_{sc} = 5 m/s

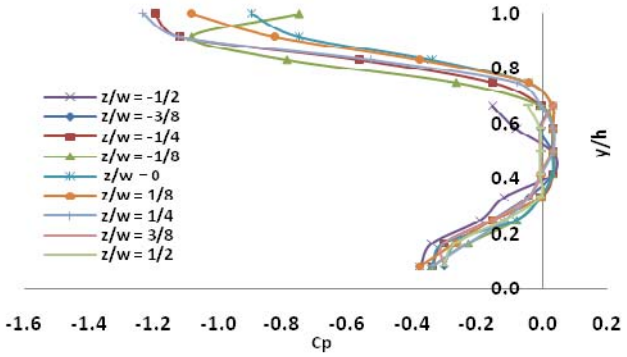

(c). Suction velocity, U_{sc} = 10 m/s

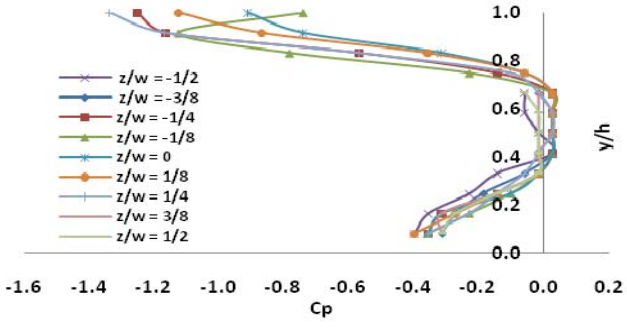

(d). Suction velocity, U_{sc} = 15 m/s

Fig 4. Pressure coefficient distribution with various suction velocity in the rear part of the reversed Ahmed body

Table 2. The minimum value of pressure coefficient with suction

Suction velocity, U_{sc} (m/s)	Pressure Coefficien, C_p
1	-1.0097
5	-1.1488
10	-1.2339
15	-1.3372

Figures 5 (a-d) shows the effect of various blowing velocity in the rear part of the reversed Ahmed body to the pressure coefficient distribution with the upstream velocity at 16.7 m/s. The blowing velocities are 1 m/s, 5 m/s, 10 m/s and 15 m/s, respectively. By the introduction of a blowing in the rear part of the body it can be seen from Fig. 5 (a-d) that the location minimum of value of pressure coefficient shifted significantly to y/*h*= 1; z/*w*= -1/4 and y/*h* = 1; z/*h* = 1/4 in the rear side of the body for blowing velocity 1 m/s, 5 m/s and 10 m/s. For blowing velocity 15 m/s, the location minimum value of pressure coefficient at y/*h* = 11/12; z/*w* = -1/4 and y/*h* = 11/12; z/*w* = 1/4 in the rear part of the body. Table 3 summarizes the alteration of the minimum value of pressure coefficient.

Table 3. The minimum value of pressure coefficient with blowing

Blowing velocity, U_{bl} (m/s)	Pressure Coefficient, C_p
1	-0.8546
5	-0.7455
10	-0.7680
15	-0.9477

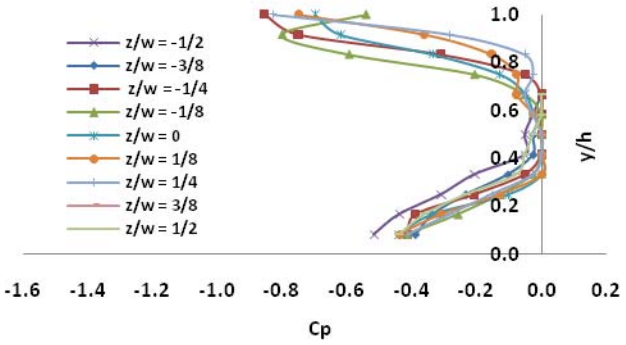

(a). Blowing velocity, U_{bl} = 1 m/s

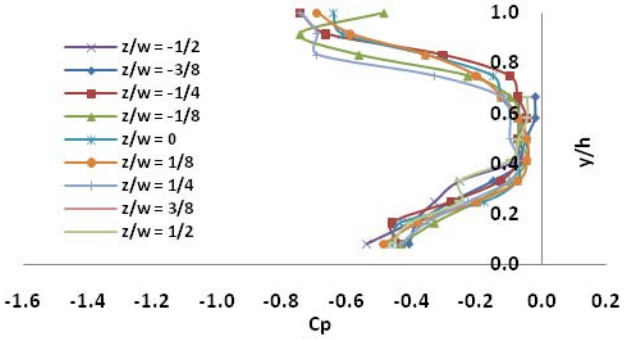

(b). Blowing velocity, U_{bl} = 5 m/s

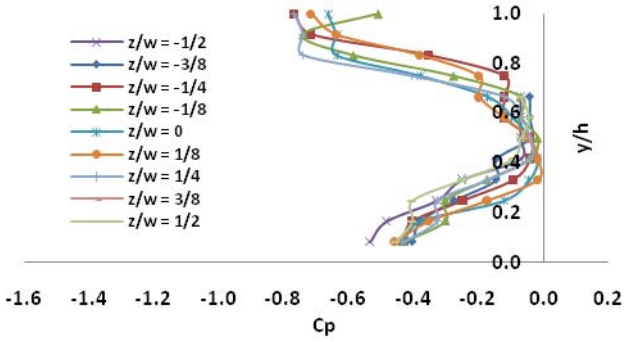

(c). Blowing velocity, U_{bl} = 10 m/s

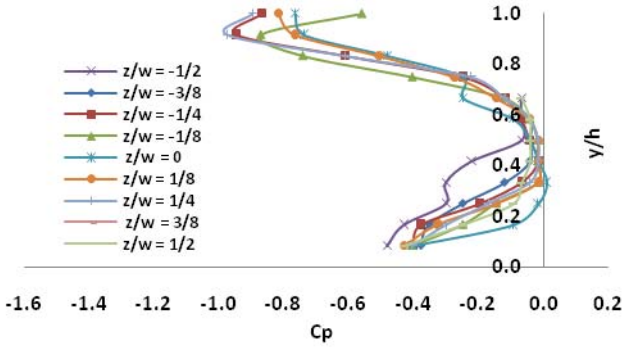

(d). Blowing velocity, U_{bl} = 15 m/s

Fig 5. Pressure coefficient distribution with various blowing velocity in the rear part of the reversed Ahmed body

B. Turbulence Intensity

The characteristics of turbulence intensity in the rear part of the van model without and with flow control are presented in Figs. (6) and (7). Fig. 6 shows the turbulence intensity without flow control in the rear part of the reversed Ahmed body with the upstream velocity at 16.7 m/s. It can be seen that the maximum value of turbulence intensity is about 1.99% without flow control.

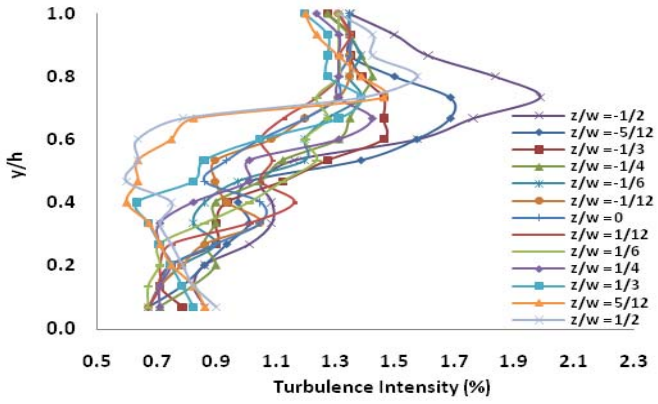

Fig 6. Turbulence intensity without flow control in the rear part of the reversed Ahmed body.

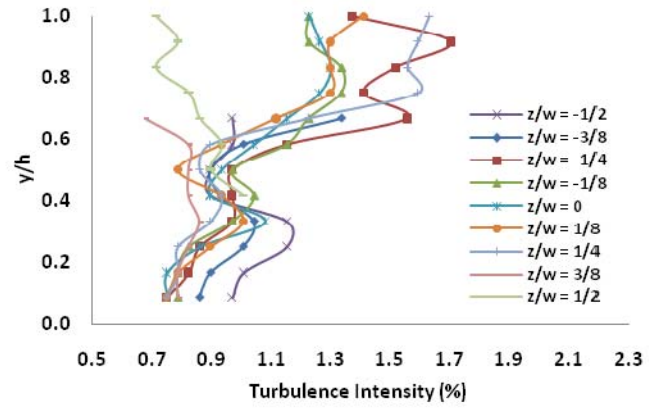

(a). Suction velocity, Usc = 1 m/s

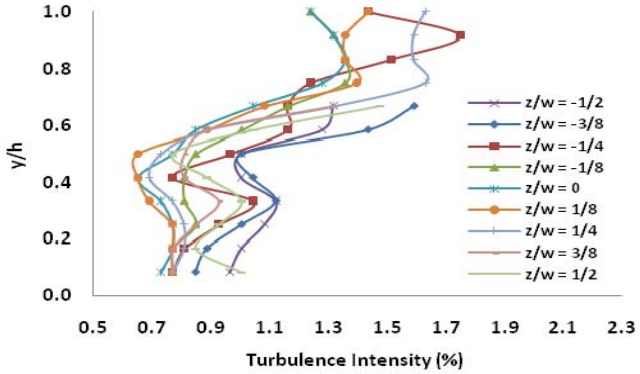

(b). Suction velocity, Usc = 5 m/s

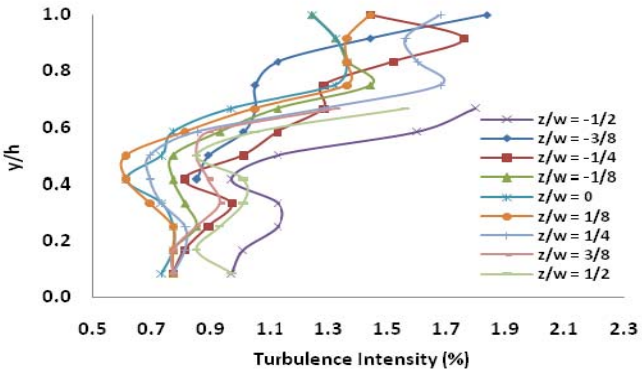

(c). Suction velocity, Usc = 10 m/s

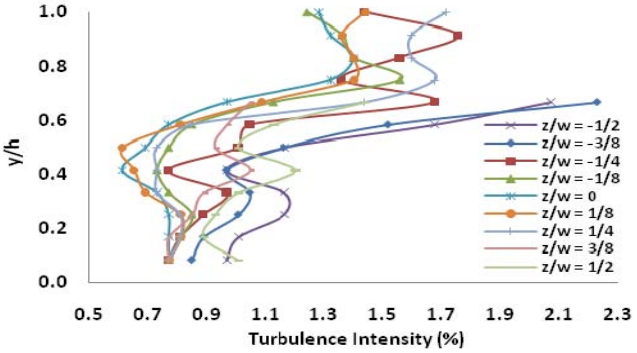

(d). Suction velocity, Usc = 15 m/s

Fig 7. Turbulence intensity with various suction velocity in the rear part of the reversed Ahmed body

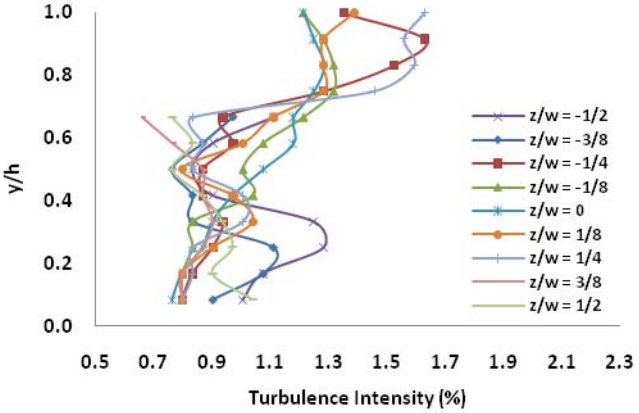

(a). Blowing velocity, U_{bl} = 1 m/s

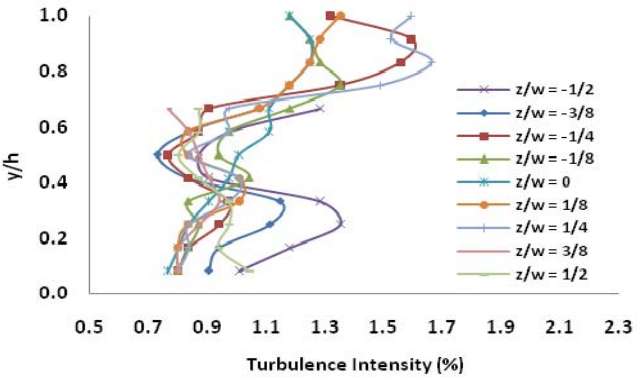

(b). Blowing velocity, U_{bl} = 5 m/s

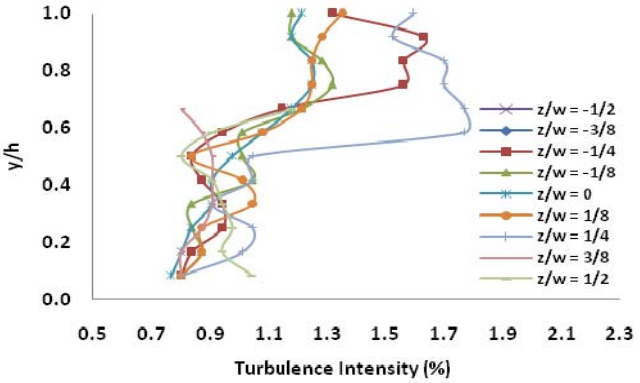

(c). Blowing velocity, U_{bl} = 10 m/s

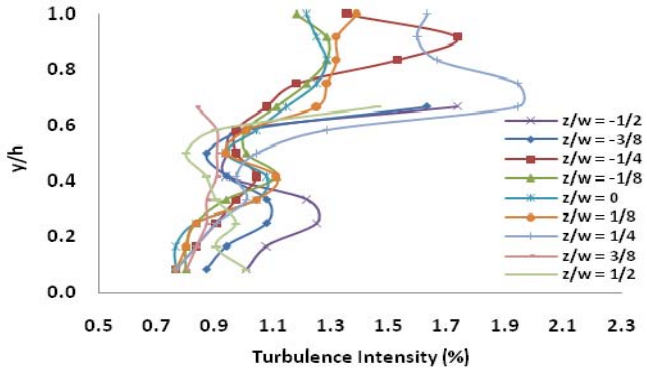

(d). Blowing velocity, U_{bl} = 15 m/s

Fig 8. Turbulence intensity with various blowing velocity in the rear part of the reversed Ahmed body

Furthermore, Fig. 7 (a-d) shows the effect of various suction velocities in the rear part of the reversed Ahmed body to the turbulence intensity distribution with the upstream velocity at 16.7 m/s. Meanwhile in Table 4 the maximum turbulence intensities under suction velocities of 1 m/s, 5 m/s, 10 m/s and 15 m/s are summarized. These results indicate that there is a decrease in the turbulence intensity by the use of suction mechanism in the rear part of the body. The largest decrease of turbulence intensity about 0.20 % is obtained at suction velocity of 5 m/s.

Table 4. The maximum value of turbulence intensity with suction

Suction velocity, U_{sc} (m/s)	Turbulence intensity, (%)
1	1.70
5	1.75
10	1.84
15	2.23

Figures 8 (a-d) describes the effect of various blowing velocities in the rear part of the reversed Ahmed body to the turbulence intensity the upstream velocity at 16.7 m/s. The blowing velocity are 1 m/s, 5 m/s, 10 m/s and 15 m/s. Meanwhile in Table 5 the maximum turbulence intensities under blowing velocities of 1 m/s, 5 m/s, 10 m/s and 15 m/s are summarized. These results indicate that there is a decrease in the turbulence intensity by the use blowing mechanism in the rear part of the body. The largest decrease of turbulence intensity about 0.36% was obtained at blowing velocity 1 m/s.

Table 5. The maximum value of turbulence intensity with blowing

Blowing velocity, U_{bl} (m/s)	Turbulence intensity, (%)
1	1.63
5	1.67
10	1.77
15	1.94

.

Generally, the turbulence intensities obtained by the use of suction and blowing are lower than those without flow control in the rear part of the reversed Ahmed body. This alteration seems to occur due to additional energy from suction and blowing which modify the flow structure so that the separation can be decreased or eliminated.

C. Aerodynamics Drag Reduction

The influences of suction and blowing are analyzed according to the aerodynamic forces applied to the geometry, with and without control. The results are presented through aerodynamic drag reduction with respect to the reference configuration (without control). The mean drag coefficients, obtained at different velocities of suction and blowing are indicated in Figures 9 and 10, respectively. In the figures, the drag reductions obtained with respect to the reference configuration (without control) are also indicated.

From Fig. 9 in the first phase, the control performance increase very rapidly with the suction velocity. The reduction obtained are 14.70 % for U_{sc} = 0.06U_o and 15.83 % for U_{sc} = 0.30U_o. These results suggest significant modifications in the flow topology for U_{sc} < 0.30 U_o. Conversely, during the second phase in fig. 9, the drag shows tendency to increase and the reduction obtained are 15.83% for U_{sc} = 0.30U_o and 14.53% for U_{sc} = 0.90U_o. Hence, from Fig. 9 it can be indicated that there is an optimum suction velocity to obtain drag reduction i.e. U_{sc} = 0.30U_o.

Closer insight to Fig. 10 in the first phase, the control performance increase very rapidly with the blowing velocity. The reduction obtained are 14.38% for U_{bl} = 0.06U_o. These result suggest significant modifications in the flow topology for U_{bl} < 0.06U_o. Conversely, during the second phase in Fig. 10, the drag show a tendency to increase and the reduction obtained are 14.38% for U_{bl} = 0.06U_o and 11.32% for U_{bl} = 0.90U_o. Hence, Fig. 10 indicates that there is an optimum blowing velocity to achieve maximum drag reduction i.e. U_{bl} = 0.06U_o

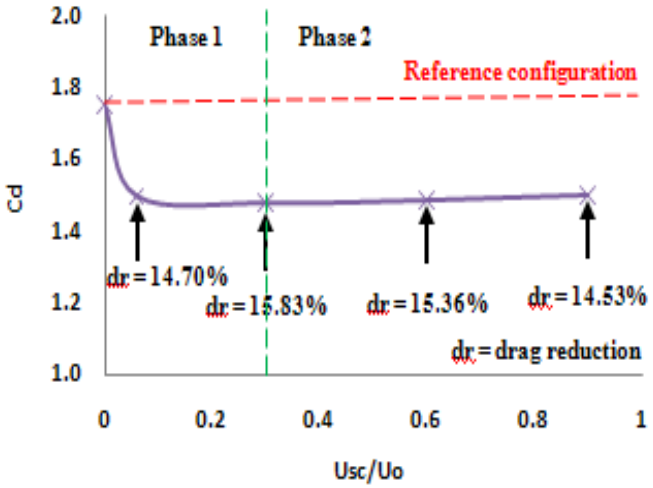

Fig 9. Drag coefficient as a function of suction velocity.

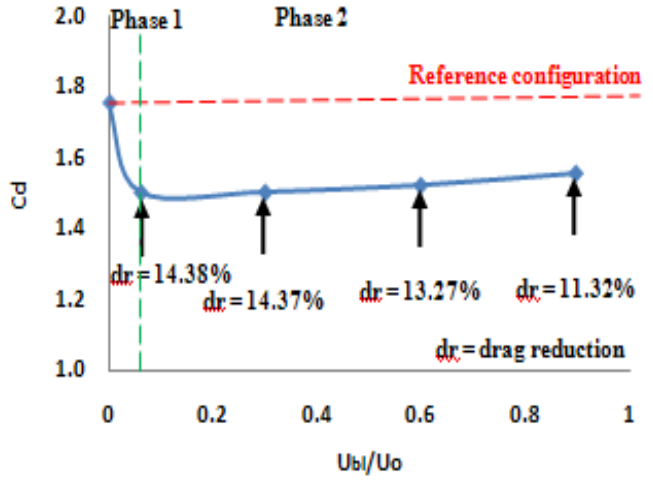

Fig 10. Drag coefficient as a function of blowing velocity.

Generally, by comparing the results obtained from the use of suction with those from the use of blowing in the rear part of the reversed Ahmed body, it can be figured out that the drag reductions obtained by suction is greater than by blowing.

IV. Conclusion

An active flow control solution by suction and blowing are tested to reduce the aerodynamic drag on reversed Ahmed body. The maximum drag reductions associated with these modifications are close to 15.83% and the increase of suction velocity increase at $U_{sc} > 0.30U_o$ does not improve such a reduction significantly. Likewise, the drag reductions decrease when the suction velocity diminishes below $0.30U_o$. In the other hand, in case of blowing in rear side on reversed Ahmed body, the drag reduction are close to 14.38% and the increase of blowing velocity at $U_{bl} > 0.06U_o$ does not improve such a reduction significantly. Moreover, the drag reductions decrease when the blowing velocity diminishes below $0.06U_o$.

The present study also show that this is a good test case for further development. In addition, the results presented in this paper give information about potential of active flow control by suction and blowing in the automobile industry. The results should, however, be corroborated by experimental results and tested on real car flow configuration.

Acknowledgment

The authors would like to thank Mr. Freddy Lay, Mr. Andre Grivanzy and Mr. Ahmad Tri Ageng.S for helping the preparation of computation facilities.

References

[1] "World Energy Outlook 2007", *Executive Summary, China and India Insights, International Energy Agency IEA*, 2007.
[2] M. Gad-El-Hak, "Modern developments in flow control", *Appl Mech Rev.* vol. 1996, no. 9, pp. 365–379, 2006.
[3] H.E. Fieldler, and H.H. Fernholz, "On the management and control of turbulent shear flows", *Prog Aero Sci*, vol. 27, 1990.
[4] C.H. Bruneau, and I Mortazavi. "Numerical modelling and passive flow control using porous media", *Comput Fluids*, vol. 37, no. 5, 2008.
[5] A.Roshko, and K. Koenig, "Interaction effects on the drag of bluff bodies in tandem", In: Sovran G, Morel T, Mason WT, editors. *Symposium on aerodynamic drag mechanisms of bluff bodies and road vehicles*, Plenum Press, 1978.
[6] P.A. Krogstad, and A. Kourakine, "Some effects of localized injection on the turbulence structure in a boundary layer", *Phys Fluids*, vol.12, pp. 2990–2999, 2000.
[7] Park J, Choi H, "Effects of uniform blowing through blowing or suction from a spanwise slot on a turbulent boundary layer flow", *Phys Fluids* vol. 11, pp. 3095–3105, 1999.
[8] M. Sano, and N. Hirayama,"Turbulent boundary layer with injection and suction through a slit", *Bull JSME,* vol. 28, pp. 807–814, 1985.
[9] T. Ivanic., and P. Gilliéron.," Reduction of the Aerodynamic Drag Due to Cooling System: An Analytical and Experimental Approach", *SAE Paper*, No. 2005 -01-1017, 2004.
[10] M. Roumeas, P. Gillieron, and A. Kourta, "Drag Reduction by Flow Separation Control on a Car after Body", *International Journal for Numerical Method in Fluids*, vol. 60, pp. 1222-1240, 2009.
[11] M. Roumeas, P.Gillieron, and A. Kourta, " Separated flow around the rear window of a simplified car geometry", *Journal of Fluids Engineering* , vol. 130, 2008.
[12] S.R. Ahmed, G. Ramm and G. Faltin, "Some salient features of the time-averaged ground vehicle wake", *SAE technical paper series*, no. 840300, Detroit, 1984.
[13] User's Guide Manual of Fluent 6.3.2, September 2006